Iraqi Journal of Oil & Gas Research

Journal homepage: https://ijogr.uotechnology.edu.iq/

Title Experimental and Optimization of Process Variables for Heat Transfer Coefficient in Bubble and Slurry Bubble Column Reactor with U-shaped heat-exchanging Tubes using Response Surface Methodology (RSM)

[1]Dalia S. Makki, [2]Hasan Sh. Majdi, [1]Amer A. Abdulrahman, [1]Abbas J. Sultan, [1]Bashar J. Kadhim, [3]Muthanna H. Al-Dahhan*

[1] Department of Chemical Engineering, University of Technology-Iraq, Baghdad, Iraq
[2] Department of Chemical Engineering and Petroleum Industries, Al-Mustaqbal University, Babylon, Iraq.
[3] Department of Chemical and Biochemical Engineering, Missouri University of Science and Technology (MS&T), Rolla, MO, United states.

Article information

Article history:
Received: August, 02, 2024
Revised: September, 24, 2024
Accepted: September, 29, 2024
Available online: October, 04, 2024

Keywords:
Fischer Tropsch,
bubble/slurry column,
heat-exchanging tubes.

Corresponding Author:
Dalia S. Makki
daliasaady1986@gmail.com

Abstract

This study involves designing and constructing a simulated Fitcher-Tropich bubble column reactor (FTBCR) that features real vertical U-shaped heat-exchanging tubes. This work investigates the influence of incorporating a real heat exchanger into a bubble and slurry bubble column (BC and SBC). The investigations were conducted in a (0.15 m) inner diameter Plexiglas (BCR) with varying gas flow rates ranging from (0.14m/s to 0.35m/s). To replicate the industrial (FTBCR), a real heat exchanger was vertically installed, occupying 25% of the column cross-section, and comprised 18 copper tubes, each with a diameter of (0.016 m). Glass beads represented the solid phase with an average size of 150 μm, which were loaded to a maximum volume of 40%. Furthermore, this investigation employed an advanced heat transfer technique to quantify the impact of the cooling tubes and solid particles on the local instantaneous heat transfer coefficient (LIHTC) to improve the quantification and understanding of the heat transport in this reactor. The investigations were conducted at three axial locations (H/D = 2, 3, and 4) and six radial sites along the column's diameter (±0.18, ±0.46, and ± 0.74). The results indicated that the (LIHTC) exhibited a substantial decrease as the gas flow rates increased at all radial and axial positions. Moreover, the (LIHTC) in the central zone increased by approximately 82% in comparison to the near the wall in the two and three phases. The model's validation was assessed by comparing the predicted and experimental values of (LIHTC) using Minitab software and response surface methodology

(RSM). The results were consistent with the experimental results. The regression model achieved for (LIHTC) in both the two and three phases (BCR) was (R^2) (95.90) and (97.49), respectively.

DOI: http://doi.org/10.55699/ijogr.2024.0402.1075 , Department of Oil and Gas Engineering, University of Technology-Iraq

1. Introduction

The significant growth of the global economy, as well as the rise in the international oil price and the growing world population, have significantly increased the world's energy and environmental concerns [1][2]. In addition to the depletion of limited resources due to population growth and rising living standards, there is also a need for energy and depleted natural resources [3][4]. Increased interest has been seen in developing highly efficient gas-to-liquid (GTL) processes due to the decrease in light crude reserves and the rising demand for diesel and jet fuel [5][6][7]. Slurry bubble column reactors ($SBCR_S$) offer several advantages for (GTL) processes, including the potential for very high heat transfer levels, which allows for high heat transfer coefficients (HTC) even with high solids loading suspended in the liquid [8][9]. (SBCRs) also help to prevent temperature excursions in highly exothermic reactions and provide better control of temperature within the reactor [10][11]. Additionally, a heat exchanger inside the reactor allows for clean water production by enabling near-adiabatic operation [12][13][14]. While heat generated by the syngas is transferred to the surrounding environment, leading to a depletion of heat, concerns remain for highly exothermic reactions, such as the Fischer-Tropich (FT) reaction, which can lead to the combustion of syngas and elevated temperatures inside the reactor [15][16]. It is important to explore alternative ways to improve the efficiency and sustainability of (HTC). Numerous researchers have used heat exchanger tubes with single-phase liquid flow, fixed or floating catalyst systems [17], and reacting solid particles [18][19], among other methods. Articles provided detailed information on flow regime maps single or two-phase flow [20], boiling mechanisms, heat transfer coefficients [21], viscosity and solute concentration effects [22], column and geometry types, and tube orientations [23].

Our survey shows no prior research has been conducted to optimize design and process variables for (LHTC) using (RSM). Therefore, the present work aims to determine and optimize the (HTC) and identify the process variables that affect efficiency and physical properties, considering stability, safety, and substance ability. Furthermore, identify the heat transfer parameters, the process variables governing the heat transfer, and the effect of changing these parameters, and provide a guide design engineers can use to achieve the best design and operational conditions. Also, to effectively disperse solid particles and gases in a liquid within the compressed gas injection under pressure for two different types of reactors (BC and SBC). By conducting these analyses, suitable controls for achieving more uniform conditions of particles, gases, and liquids within the reactor are identified. As a result, the reactor's performance in terms of heat transfer should enable more accurate calculations.

2. Experimental setup

As seen in Figure 1. (FT-BCR) experimental setup was created and built using an actual heat exchanger to accurately assess the impact of tube arrangement and real U-shaped heat exchanger tubes on the local and overall heat transfer coefficient. The (BC) has a diameter of 0.15 m and a height of 1.83 m. In this study, glass beads measuring 150 µm in size and having a density of 2500 kg/m³ were employed to simulate the fine catalyst used in an industrial FT reactor. The loading of these glass beads was up to 40% by volume. A thermal tank with a controller was fitted to imitate the performance of U-shaped heat exchanger tubes used in industrial settings. This system circulated heated liquid (50°C) through the tubes, with hot water being pumped into the tubes and returned to the heater in a recycling manner. The (BC) was supplied with cold liquid (10°C), which was also recycled, via a pump from a chiller tank that was furnished with a controller to regulate the water temperature.

The compressed air is introduced into the column by a gas distributor made of porous polyethylene. The gas distributor has a thickness of (12.7 mm) with a pore size of (50 µm), and contains (137) holes. This gas distributor ensures that the air is distributed evenly and supports the solid particles' weight. The distributor plate was positioned (10 cm) above the bottom end of the vertical tubes. The compressed air is directed via a calibrated polycarbonate panel flowmeter to achieve the necessary flow rates for industrial purposes, including bubbling, slugging, and churning turbulent flow regimes. Data has been collected experimentally to assess the effect of tube configuration on the (LIHTC) within a range of superficial gas velocity (U_g) values (0.14 - 0.35 m/s).

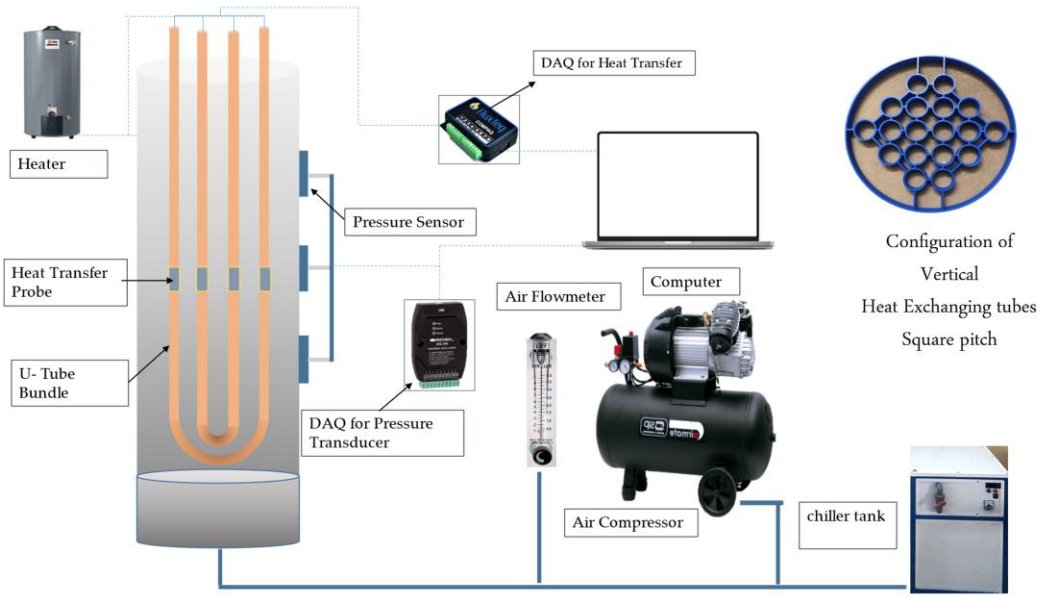

Figure 1: Schematic layout of the bubble column including vertical industrial U-shaped heat exchanger tubes.

The heat-exchanging tubes installed within the (BC) covered 25% of its cross-sectional area. These tubes were designed to simulate the specifics of an industrial reactor, as shown in Fig.2. They were made of eighteen copper tubes, each measuring 1.90 m in height and 0.016 m in diameter. A square-pitch configuration was designed to arrange the tube bundles within the (BC) following specific layout standards.

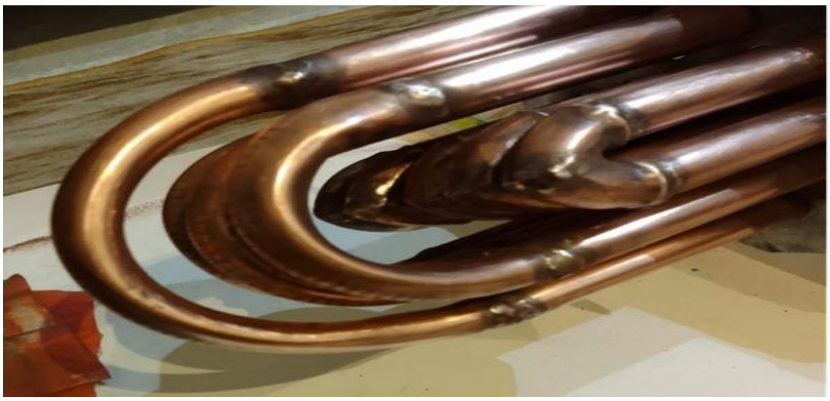

Figure 2: Photo of the U-shaped heat exchanger.

2.1 A sophisticated technique of heat transfer

Advancements in technology have enabled the utilization of attachable heat flux sensors to accurately measure and monitor the surface temperature of tubes, heat flux, and subsequently, the (LIHTC) with great sensitivity in real-time. These technological improvements have also facilitated the creation of a rapid-response heat transfer method to calculate (LIHTC) in the (SBC) that is equipped with tube bundles.

The (FluxTeq LLC) sensor, manufactured in Blacksburg, USA (VA24060-6370), is highly skilled at accurately monitoring both surface temperature and heat flux rate. For this study, a total of eighteen sensors were strategically affixed to the U-shaped heat exchanger tubes along their height and diameter at various points using thermal adhesive glue. This configuration consisted of three sensors that were coupled in both an axial and radial manner within each tube.

The bulk temperature was measured at various points within a (10 cm) distance of each of the four type T thermocouples placed above the distributor plate. The (PHFS) heat flux and integrated temperature sensors were read and recorded using the (PAQ) Heat Flux and Thermocouple Data Acquisition Instrument (FluxTeq LLC, Blacksburg, VA240606370, USA).

The device is equipped with eight variation channels and can manage up to four complete (PHFS) sensors., each of which measures both heat flux and surface temperature. Channels 1, 3, and 7 of these data-collecting devices were designed to receive heat flux leads, whereas channels 2, 4, and 6 were designated to receive the corresponding T-type thermocouples.

This data reader's software generates temperature and heat flux charts for each channel. Displaying and importing the data into the MATLAB program allowed us to instantly calculate the (LHTC) by measuring the heat flux per unit area, the temperature difference between the surface and bulk temperatures, and other factors, as shown in Eq. (1) [13]:

$$h_{i(t)} = \frac{q_{i(t)}}{T_{S(t)} - T_b} \qquad \text{.....(1)}$$

Where $h_{i(t)}$= instantons local heat transfer coefficient "W/m^2. °C"

$q_{i(t)}$ = instantons heat Flux per unit area "W/m^2"

$T_{S(t)}$ = surface temperature °C

T_b = bulk temperature °C

To confirm the replicability of the advanced heat transfer technology, the measurements of the (LHTC) were duplicated twice, with a seven-day interval, for each gas velocity. It is crucial to note that every value of the (LHTC) was reproduced three times to minimize the errors of experimental in the data. Thus, the results only included the mean values of the (HTC).

Furthermore, all measurements in this work are read and recorded in the absence of glass beads by means two-phase system (air-water) system and in the presence of glass beads or a three-phase system (air-water-glass beads), to investigate the impact of solid particles and superficial gas velocities with U-shaped heat-exchanging tubes on (LIHTC) at several radial sites along the column's diameter (r/R = ±0.18, ±0.46, and ± 0.74) and three axial locations (H/D = 2, 3 and 4)

2.2 Optimization and Modelling of Processes

The systems' efficacy and the yield of the processes must be enhanced without an increase in cost. Optimization is employed for this objective carried out by using Response Surface Methodology (RSM)[24]. (RSM) is a set of statistical and mathematical techniques that are valuable for the development, improvement, and optimization of processes [25][26]. These processes involve a response of interest that is influenced by multiple variables, and the objective is to optimize this response. It is a statistical procedure employed to establish several experiments in various physical and chemical processes.

The experiments were conducted using the software) MINITAB 19). The current research investigated the optimization of several different parameters., (radial position; axial positions, and superficial gas velocity) to predict the maximum heat transfer coefficient in two and three-phase systems. Furthermore, the interaction effect of parameters has been investigated. Design of experiment (DOE) is a statistical model that is used. It is an optimized design for fitting quadratic models with equal predictability in all directions from the center. The maximum and minimum levels of the experimental design are given in Table (1). The experimental designs are presented in Table (2) for the two-phase system and Table (3) for the three-phase system. Response surface methodology (RSM) designed by Box-Behnken (BB) was used, which consists of 3 independent variables containing 20 experiments.

Table 1: Minimum and maximum values of parameters.

Parameters	**Code**	**Low level**	**High level**
Radial position	r/R	0.18	0.74
Axial position	H/D	2	4
Superficial gas velocities	Ug	0.14	0.35

Table 2: Design of experiment of two-phase system.

r/R	**H/D**	**U_g**	**h**
0.74	2	0.14	5083
0.74	2	0.21	4093
0.74	2	0.28	3290
0.74	2	0.35	2049
0.74	3	0.14	6407
0.74	3	0.21	4393
0.74	3	0.28	3759
0.74	3	0.35	2507
0.74	4	0.14	885.45
0.74	4	0.21	2729.05
0.74	4	0.28	1944.45
0.74	4	0.35	2023.32
0.46	3	0.14	3767
0.46	3	0.21	3197
0.46	3	0.28	2711
0.46	3	0.35	1763
0.18	3	0.14	876.08
0.18	3	0.21	2707
0.18	3	0.28	1970
0.18	3	0.35	1990

Table 3: Design of experiment of three-phase system.

r/**R**	**H/D**	$\mathbf{U_g}$	**h**
0.74	2	0.14	4109.07
0.74	2	0.21	3085.79
0.74	2	0.28	2216.40
0.74	2	0.35	1051.02
0.74	3	0.14	3718.56
0.74	3	0.21	2709.0
0.74	3	0.28	2225.41
0.74	3	0.35	1195.72
0.74	4	0.14	585.19
0.74	4	0.21	1706.68
0.74	4	0.28	1031.17
0.74	4	0.35	1004.92
0.46	3	0.14	2675.50
0.46	3	0.21	2102.55
0.46	3	0.28	1720.99
0.46	3	0.35	782.548
0.18	3	0.14	639.98
0.18	3	0.21	1904.29
0.18	3	0.28	1596.81
0.18	3	0.35	466.53

3. Results and Discussions

3.1 The effect of (U_g) on the average (LHTC) at radial sites in the two-phase system

As shown in Figure (3) the maximum average (LHTC) values by moving towards the center region at each (U_g).

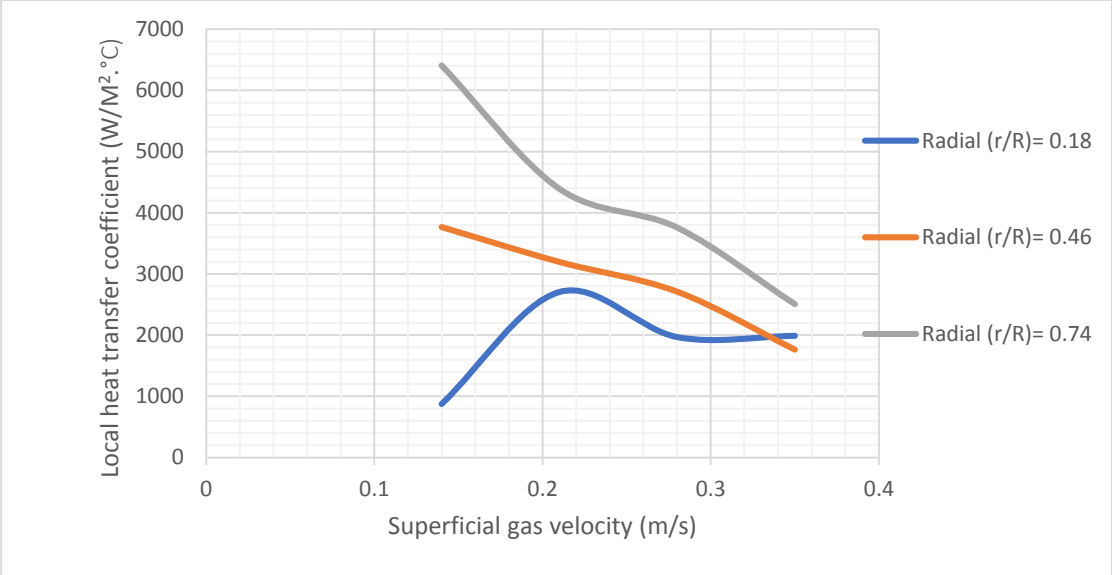

Figure 3: Effect of the superficial gas velocity on the average (LIHTC) at different radial sites in the two-phase system.

For example, the average (LHTC) at (U_g = 0.14, 0.21, 0.28, and 0.35 m/s) in the center region (r/R = 0.74) was higher than at sites (r/R = 0.18 and r/R = 0.46) by (86% and 41%), (38% and 27%), (47% and 27%) and (20% and 29%). This is because dense heat exchange internals in the center influence the distribution of bubble sizes, increase the velocity of the liquid, decrease liquid back mixing, and significantly improve the rate at which the bubbles split up. Additionally, in deep churn-turbulent at high superficial gas velocity, the bubble's coalescence and breakup rates come to a balance and hence bubble size and bubble rise velocity reach close to a plateau[16][27].

3.2 The effect of (U_g) on the average (LHTC) at axial sites in the two-phase system

Figure (4) illustrates the average of (LHTC) at (U_g = 0.14, 0.21, 0.28, and 0.35 m/s) in the center region (H/D = 3) was higher than at sites (H/D = 2 and H/D = 4) by (86% and 20%), (35% and 6%), (47% and12%) and (16% and 18%). This is because the coalescence and disintegration rates of the bubbles in deep churn-turbulent at high superficial gas velocities reach a balance, resulting in bubble size and bubble rise velocity approaching a plateau [28]. Additionally, the dynamics and properties of the bubbles may be influenced by the internals. Concurrently, the distribution of the heat transfer was heterogeneous near the wall region as a result of the progressively dense bubble at the wall [29].

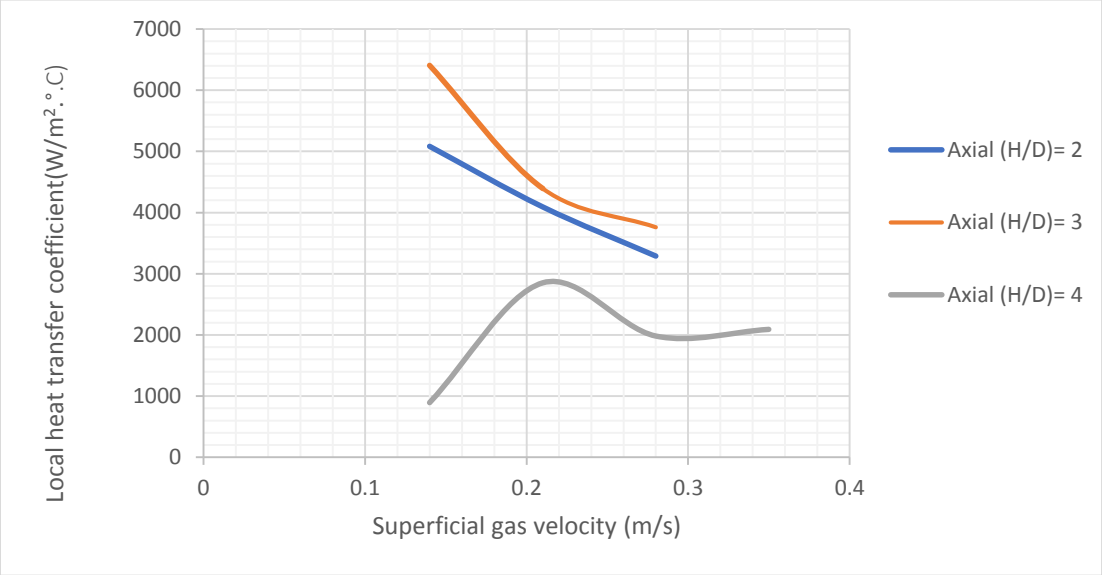

Figure 4: Effect of the superficial gas velocity on the average (LIHTC) at different axial sites in the two-phase system.

3.3 The effect of (U_g) on the average (LHTC) at radial sites in the three-phase system

Figure (5) demonstrates that the average (LHTC) decreased as superficial gas velocity increased and the maximum average (LHTC) values by moving towards the center region at each (U_g).

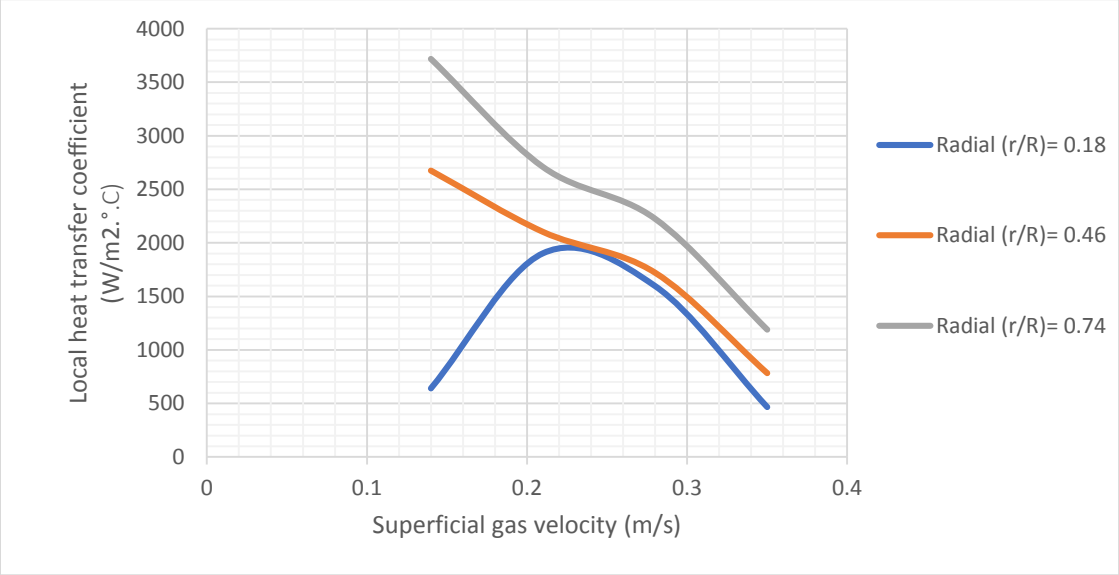

Figure 5: Effect of superficial gas velocity on the average (LIHTC) at different radial sites in the three-phase system.

Furthermore, the average (LHTC) at (U_g = 0.14, 0.21, 0.28, and 0.35 m/s) in the center region (r/R= 0.74) was higher than at sites (r/R= 0.18 and r/R= 0.46) by (82% and 28%), (29% and 22%), (28% and 22%) and (60% and 34%). As a result of numerous factors related to the hydrodynamics and flow patterns within the column. Furthermore, the central region is frequently subjected to more intense turbulence and mingling than the region close to the walls.

Turbulence enhances the mingling of the liquid and solid phases, thereby improving convective heat transfer [30]. The convective (HTC) decreased as the level of turbulence decreased near the wall. Also, a decreased (LHTC) is

the consequence of the observed pattern, which is caused by the complex interactions between solid; gas; and liquid particles within the column [31].

3.4 The effect of (U_g) on the average (LHTC) at axial sites in the three-phase system

Figure (6) shows that the average (LHTC) exhibited varied behavior. Specifically, at the first site (H/D = 2), the average (LHTC) was greater at (U_g = 0.14 and 0.21 m/s) compared to sites (H/D = 3 and 4) with differences of 9% and 85%, and 12% and 44% respectively.

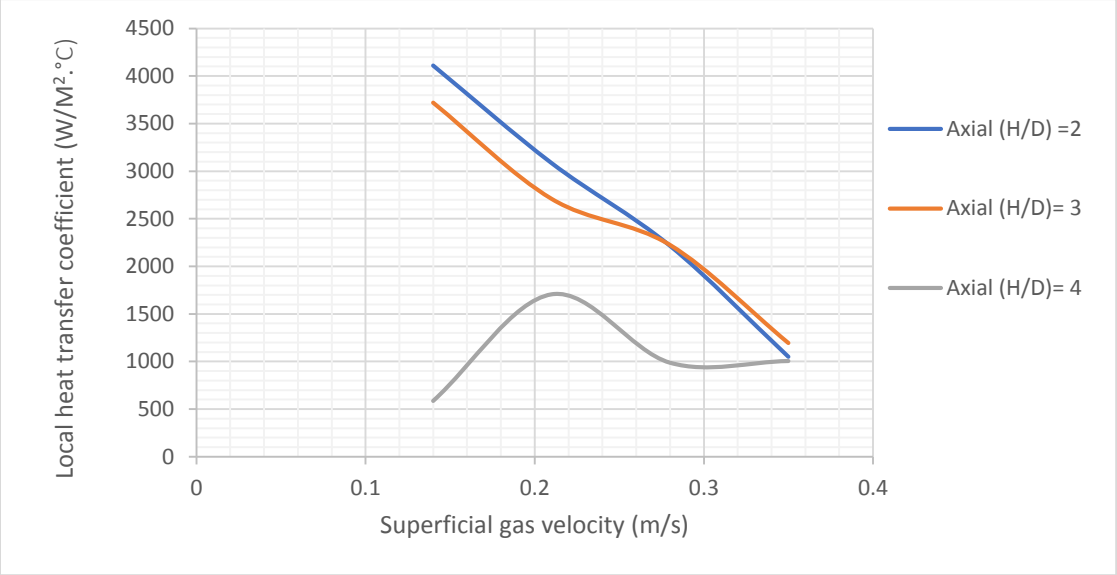

Figure 6: Effect of superficial gas velocity on the average (LIHTC) at different axial sites in the three-phase system.

Subsequently, the average (LHTC) values were almost equal at (H/D = 2 and 3), with (U_g = 0.28 and 0.35 m/s). This is due to the possibility of solid particles displaying an uneven distribution along the radial axis. Near the walls, the concentration of solid particles may be reduced due to a decrease in mixing and turbulence. Generally, solid particles often enhance heat transfer since they have better thermal conductivity [32].

Furthermore, a non-homogeneous response was detected at position (H/D = 4) as a result of foam production. There has been an increase in the churn flow, which has led to the production of foam and the mixing of liquid with the gas phase [33]. Moreover, the movement and scattering of the particles within the bed, together with the opposition displayed by the particles when the vertical heat exchanger tubes are present in the reactor [34]. Moreover, the collective impact of bubble dynamics, turbulence, flow regimes, and internal design.

3.5 Statistical Modeling and Optimization

Response surface methodology (RSM) plays a crucial role in the design, development, and formulation of new products and in enhancing the design of existing products. It determines the impact of the independent variables, either individually or in combination, on the processes [26].

3.6 Regression Model

The modeling findings have been adjusted to match the second-order polynomial equation

according to Box-Behnken (BB) model equation 4-4.

$$Y = B_\circ + \sum_{i=1}^{3} B_i X_i + \sum_{i=1}^{3} B_{ii} X_i^2 + \sum_{i=1}^{3} \sum_{j=i+1}^{3} B_{ij} X_i X_j \quad \ldots\ldots (2)$$

In this equation, Y is the response,

β_0 is a constant,

βi is a linear coefficient,

βii is the quadratic coefficient,

βij is the interaction coefficient,

Xi and Xj are independent variables.

The model's accuracy has been assessed using the regression coefficient (R^2).

Regression model equations for (LIHTC) are expressed in equations (3 and 4), which show the relation between parameters and response.

$$h = -3828 + 166\left(\frac{r}{R}\right) + 6326\left(\frac{H}{D}\right) - 16422U_g + 6628\left(\frac{r}{R}\right)^2 - 1268\left(\frac{H}{D}\right)^2 + 8903(U_g)^2 - 12629\left(\frac{r}{R}\right)U_g + 2657\left(\frac{H}{D}\right)U_g \quad \ldots\ldots (3)$$

$$h = 4086 - 222\left(\frac{r}{R}\right) + 872\left(\frac{H}{D}\right) - 16113\,U_g + 2636\left(\frac{r}{R}\right)^2 - 387\left(\frac{H}{D}\right)^2 - 5054(U_g)^2 - 4462\left(\frac{r}{R}\right)U_g + 3702\left(\frac{H}{D}\right)U_g \quad \ldots\ldots (4)$$

Contour plots represent these equations. The response of the (LIHTC) can be shown as a three-dimensional contour plot, as depicted in Figures (7 and 8) for two and three phases respectively. The (LIHTC) is plotted against the three parameters to identify the optimum parameters.

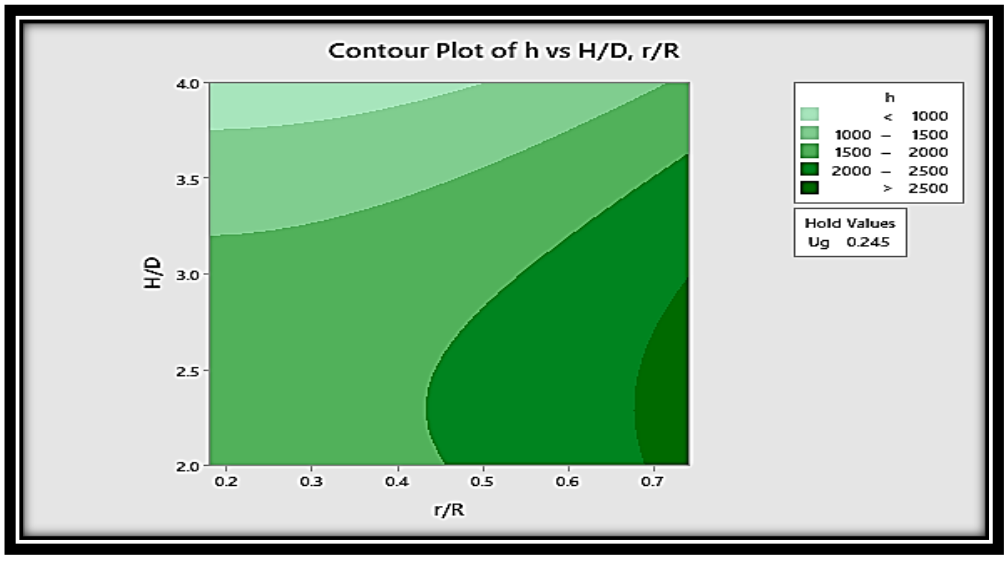

(A)

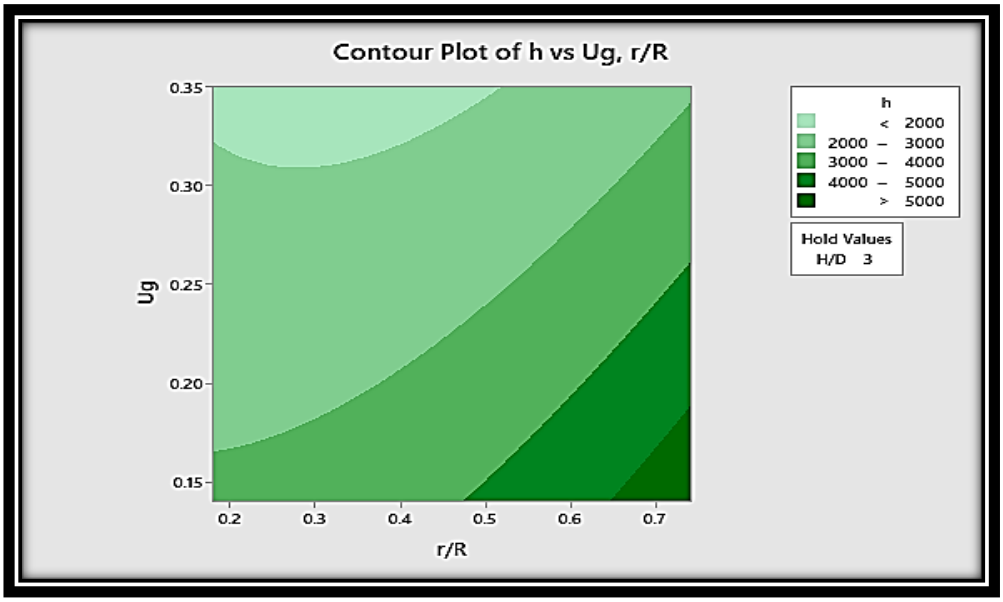

(B)

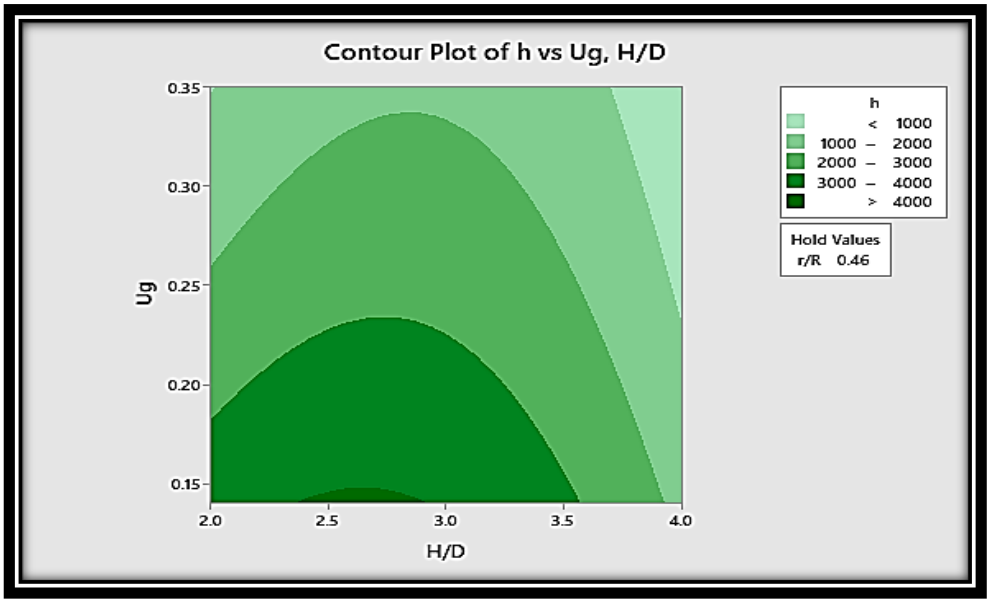

(C)

Figure 7: Effect of three independent variables on (LIHTC) in the two-phase system

A- Effect of (H/D) and (r/R); B- Effect of (U_g) and (r/R); C- Effect of (U_g) and (H/D)

Figure (7) illustrates the highest average values of (LHTC) as it moves towards the center region both axially and radially for each (U_g), which can be ascribed to the influence of internal factors on the dynamics and characteristics of the bubble. At the same time, near the wall region, the heat transfer distribution was heterogeneous due to an increasingly dense bubble at the wall.

In addition, in very turbulent conditions with deep churn, the rates of bubble coalescence and breakup achieve an equilibrium, resulting in a stable bubble size and rise velocity [29].

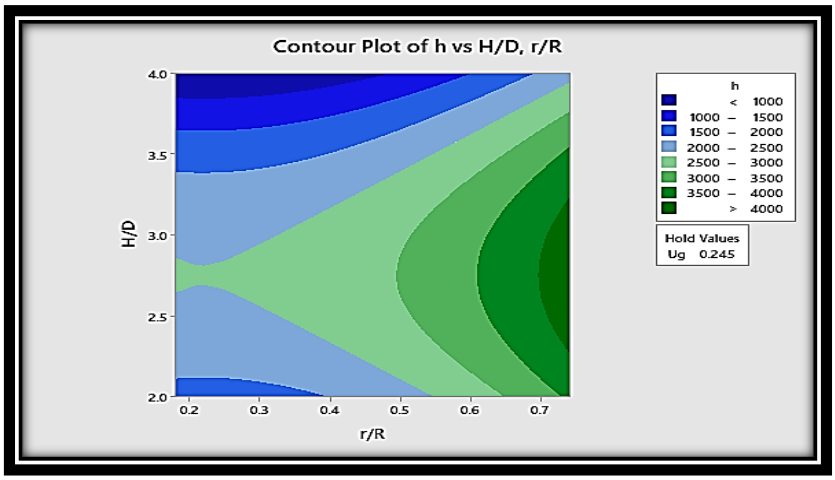

(A)

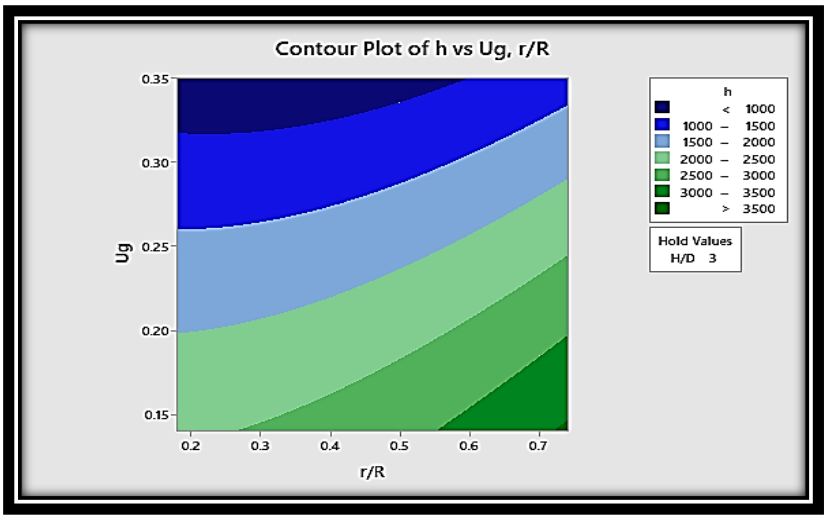

(B)

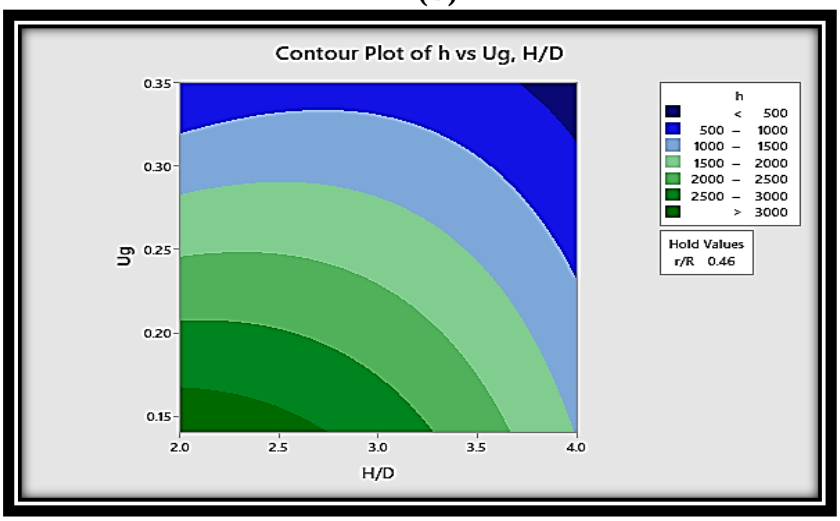

(C)

Figure 8: Effect of three independent variables on (LIHTC) in the three-phase system

A- Effect of (H/D) and (r/R); B- Effect of (U_g) and (r/R); C- Effect of (U_g) and (H/D)

Figure (8) demonstrates the average (LHTC) decreased as superficial gas velocity increased and the maximum average (LHTC) values by moving towards the center region at radial sites at each (U_g). Non-uniform behavior continues at all radial and axial sites for every (U_g), due to the solid particles that may have an uneven distribution along the radial and axial directions. The concentration of solid particles may be reduced due to a decrease in mixing and turbulence [32].

3.7 Validation of the Model

To assess the validity of the model, the predicted values were compared to the experimental values. The regression results of (LIHTC) models in two and three-phase systems indicated that the models can fit the experimental data as shown in Figures (9 and 10).

Furthermore, the (R^2) high values were (R^2) are (95.90) and (97.49) for two and three phases (BC) respectively, demonstrate the model's significant protentional for heat transfer coefficient prediction and optimization.

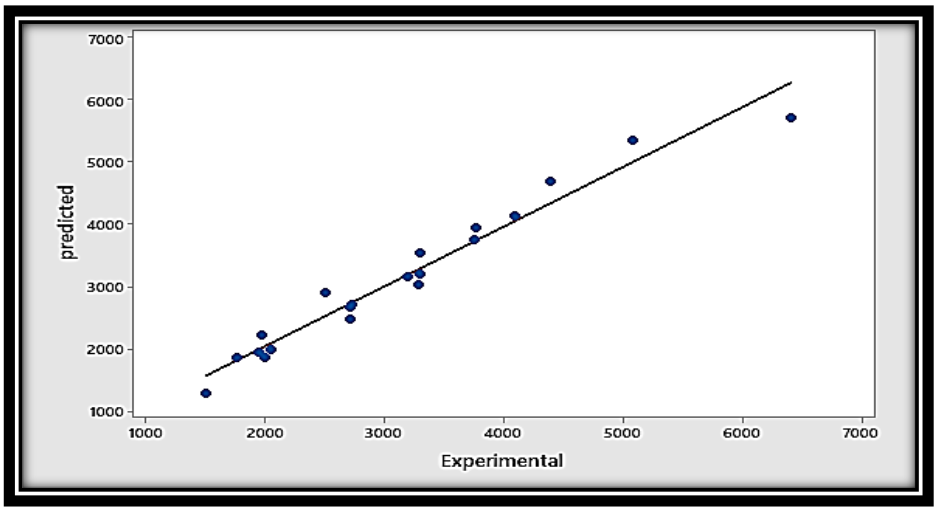

Figure 9: Scatterplot of heat transfer coefficient experimental value against predicted in the two-phase system.

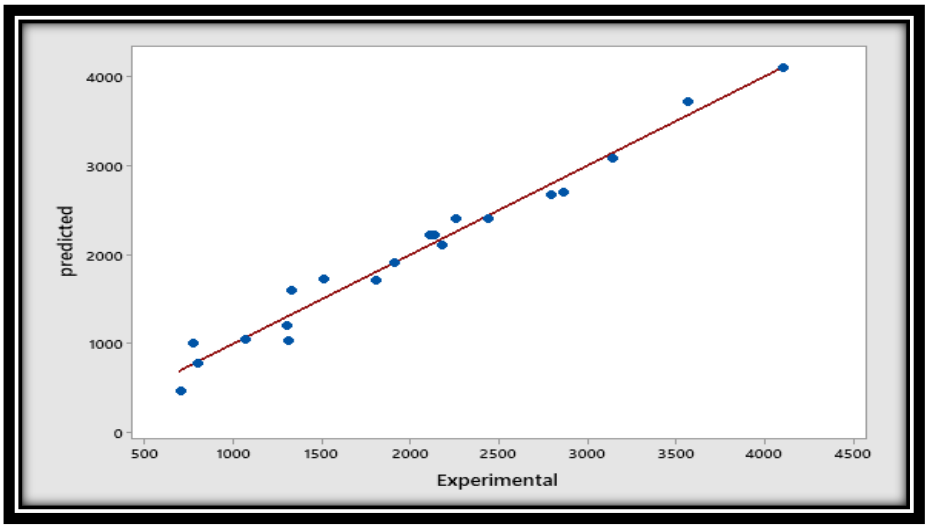

Figure 10: Scatterplot of heat transfer coefficient experimental value against predicted in the three-phase system.

3.8 Response Optimization

The response optimization identifies the optimum parameters for maximum (LIHTC) as shown in Figures (11 and 12) for two and three-phase systems (BCR) respectively. The results showed that the maximum heat transfer coefficient was (5883.52 w/m^2) in two phases (BC) at (0.74, 2, and 0.14 m/s) for the radial position (r/R), axial position (H/D), and U_g respectively.

Furthermore, in three-phase (SBC), the maximum heat transfer coefficient was (4111.97 w/m$^{2)}$ at (0.74, 2, and 0.14 m/s) for the radial position (r/R), axial position (H/D), and (U_g) respectively.

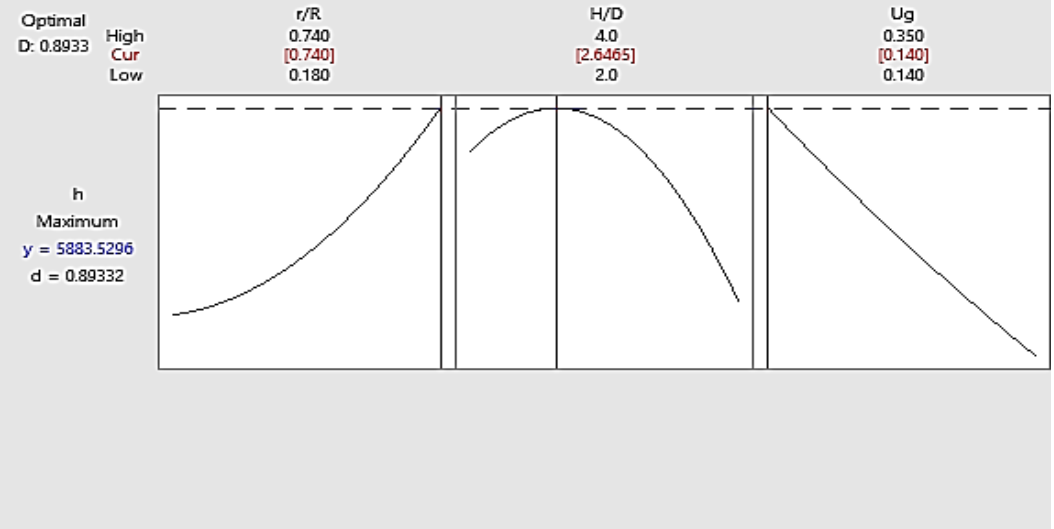

Figure 11: response optimization in the two-phase system.

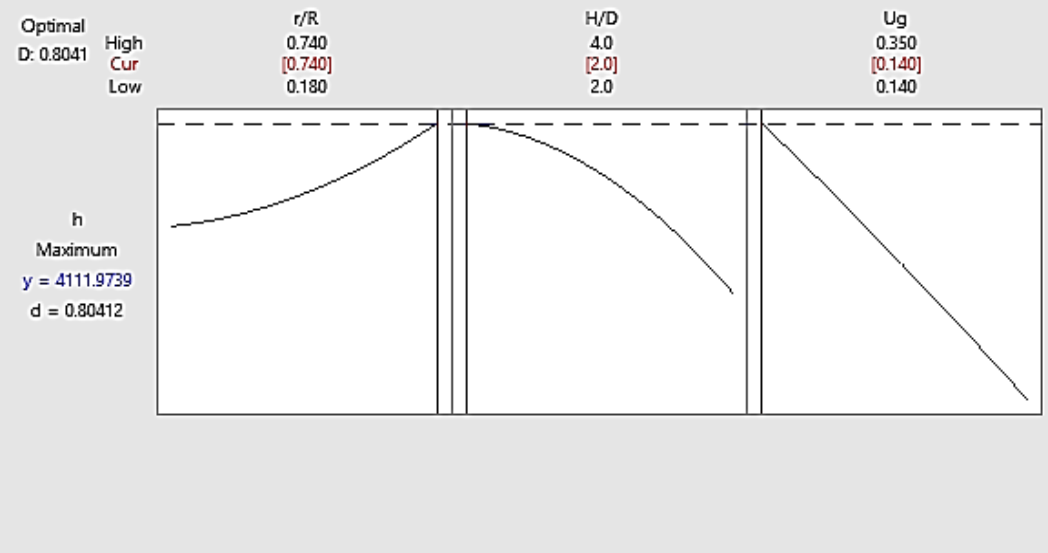

Figure 12: response optimization in the three-phase system.

4. Conclusions

A novel investigation was conducted in a simulated (FT-BCR/SBCR) to measure and optimize the (LIHTC) and identify the process variables by using the (RSM) model. Advanced heat transfer techniques were employed to obtain accurate results. The investigation focused on the impact of a genuine U-shaped heat-exchanging tube arrangement with a square pitch and the presence of solid particles at various superficial gas velocities. The results of the RSM can be used to improve heat transfer systems (heat transfer mechanisms and equipment) used in full-scale Fischer-Tropsch (FT) reactors, which are employed in industrial-scale settings, including heat exchanger tubes. On a massive industrial scale, these systems regulate and control the heat that is produced or absorbed during chemical reactions. Optimizing the design and operation of heat exchangers in Fischer-Tropsch reactors is crucial for FT synthesis because it ensures efficient heat removal or distribution, prevents hotspots, maintains reaction temperature, and supports overall reactor efficiency and stability. The comprehensive research findings from this experimental investigation can be summarized in subsections as follows:

1. The (LIHTC) was observed to decrease substantially as gas flow rates increased in all radial and axial positions.

2. The (LIHTC) decreased with increasing the gas flow rates near the wall region (±0.18). On the other hand, they have still rose with the gas flowrates at central region along the diameter of the column due to greater turbulence and mixing in comparison to the region near the walls, which improves convective heat transfer by enhancing the mixing of the liquid and solid phases.

3. Heat exchanger tubes can disrupt flow patterns, which can lead to stagnant flow or reduced velocity in areas near the walls (±0.18). As a consequence of the prevalence of these stagnant zones, the (LIHTC) has decreased due to a reduction in convective heat transfer.

4. The presence of solid particles may be reduced near the walls due to reduced mixing and turbulence. Consequently, the (LIHTC) decreases as the concentration of these particles near the walls decreases.

5. Non-uniform behavior of flow and reduce (LIHTC) can be observed at position (H/D= 4), due to the formation of foam.

References

[1] Q. Hassan *et al.*, "The renewable energy role in the global energy Transformations," *Renew. Energy Focus*, vol. 48, no. January, p. 100545, 2024, doi: 10.1016/j.ref.2024.100545.

[2] Q. Hassan, S. Algburi, A. Zuhair, and T. J. Al-musawi, "A comprehensive review of international renewable energy growth," *Energy Built Environ.*, no. September 2023, 2024, doi: 10.1016/j.enbenv.2023.12.002.

[3] S. Ovchinnikova, A. Borovkov, G. Kukinova, and N. Markina, "Environmental substantiation for the use of alternative energy sources," vol. 01007, pp. 1–6, 2021. doi.org/10.1051/e3sconf/202124401007

[4] M. Shahabuddin, T. Alam, B. B. Krishna, T. Bhaskar, and G. Perkins, "Bioresource Technology A review on the production of renewable aviation fuels from the gasification of biomass and residual wastes," *Bioresour. Technol.*, vol. 312, no. March, p. 123596, 2020, doi: 10.1016/j.biortech.2020.123596.

[5] M. Martinelli, M. Kumaran, S. Leviness, G. Jacobs, and W. D. Shafer, "An overview of Fischer-Tropsch Synthesis: XtL processes, catalysts, and reactors," *Appl. Catal. A, Gen.*, vol. 608, no. July, p. 117740, 2020, doi: 10.1016/j.apcata.2020.117740.

[6] G. R. S. Santos, O. M. Basha, R. Wang, H. Ashkanani, and B. Morsi, "Techno-economic assessment of Fischer-Tropsch synthesis and direct methane-to-methanol processes in modular GTL reactors," *Catal. Today*, vol. 371, no. July, pp. 93–112, 2021, doi: 10.1016/j.cattod.2020.07.012.

[7] A. P. Vogel, B. Van Dyk, and A. M. Saib, "GTL using efficient cobalt Fischer-Tropsch catalysts," *Catal. Today*, vol. 259, no. August, pp. 323–330, 2015, doi: 10.1016/j.cattod.2015.06.018.

[8] B. H. Davis, "Fischer-Tropsch synthesis: Overview of reactor development and future potentialities," *Top. Catal.*, vol. 32, no. 3–4, pp. 143–168, 2005, doi 10.1007/s11244-005-2886-5.

[9] T. Wang, J. Wang, and Y. Jin, "Slurry reactors for gas-to-liquid processes: A review," *Ind. Eng. Chem. Res.*, vol. 46, no. 18, pp. 5824–5847, 2007, doi: 10.1021/ie070330t.
[10] D. S. Makki *et al.*, "A Comprehensive Review of the Influence of Heat Exchange Tubes on Hydrodynamic, Heat, and Mass Transfer in Bubble and Slurry Bubble Columns," *Fluid Dyn. Mater. Process.*, vol. 19, no. 10, pp. 2613–2637, 2023, doi: 10.32604/fdmp.2023.028081.
[11] A. N. Mahmood, A. A. Abdulrahman, L. S. Sabri, A. J. Sultan, H. Shakir Majdi, and M. H. Al-Dahhan, "Flow Regimes in Bubble Columns with and without Internals: A Review," *Fluid Dyn. Mater. Process.*, vol. 0, no. 0, pp. 1–18, 2023, doi: 10.32604/fdmp.2023.028015.
[12] M. K. Al Mesfer, A. J. Sultan, and M. H. Al-Dahhan, "Impacts of dense heat exchanging internals on gas holdup cross-sectional distributions and profiles of bubble column using gamma ray Computed Tomography (CT) for FT synthesis," *Chem. Eng. J.*, vol. 300, pp. 317–333, 2016, doi: 10.1016/j.cej.2016.04.075.
[13] Z. W. Hasan *et al.*, "Experimental Investigation on Heat Transfer in A Gas-Solid Fluidized Bed with A Bundle of Heat Exchanging Tubes," " vol. 40, 09, January 2022. doi.org/10.30684/etj.v40i9.1094
[14] A. A. Jasim, A. J. Sultan, and M. H. Al-Dahhan, "Impact of heat exchanging internals configurations on the gas holdup and bubble properties in a bubble column," *Int. J. Multiph. Flow*, vol. 112, no. August 2018, pp. 63–82, 2019, doi: 10.1016/j.ijmultiphaseflow.2018.11.008.
[15] A. Jasim, ' Mine The impact of heat exchanging internals on hydrodynamics of bubble column reactor," (2016). Masters Theses. 7507.
[16] A. A. Jasim, A. J. Sultan, and M. H. Al-Dahhan, "Impact of heat exchanging internals configurations on the gas holdup and bubble properties in a bubble column," *Int. J. Multiph. Flow*, vol. 112, no. November, pp. 63–82, 2019, doi: 10.1016/j.ijmultiphaseflow.2018.11.008.
[17] N. Zheng, F. Yan, K. Zhang, T. Zhou, and Z. Sun, "A review on single-phase convective heat transfer enhancement based on multi-longitudinal vortices in heat exchanger tubes," *Appl. Therm. Eng.*, p. 114475, 2019, doi: 10.1016/j.applthermaleng.2019.114475.
[18] A. A. A. and M. F. A. H, Luma, "study on the effect of solid properties on the hydrodynamics in an ebullated Bed reactor," vol. 10, pp. 48–59, doi: 10.36909/jer.11363.
[19] S. Mahmoudi and M. W. Hlawitschka, "Effect of Solid Particles on the Slurry Bubble Columns Behavior – A Review," *ChemBioEng Rev.*, vol. 9, no. 1, pp. 63–92, 2022, doi: 10.1002/cben.202100032.
[20] Z. Sun and J. Zhu, "A consolidated flow regime map of upward gas fluidization," no. May, pp. 1–15, 2019, doi: 10.1002/aic.16672.
[21] R. S. Abdulmohsin, B. A. Abid, and M. H. Al-Dahan, "Chemical Engineering Research and Design Heat transfer study in a pilot-plant scale bubble column," *Chem. Eng. Res. Des.*, vol. 89, no. 1, pp. 78–84, 2010, doi: 10.1016/j.cherd.2010.04.019.
[22] E. M. Lakhdissi, A. Fallahi, C. Guy, and J. Chaouki, "Effect of solid particles on the volumetric gas-liquid mass transfer coefficient in slurry bubble column reactors," *Chem. Eng. Sci.*, p. 115912, 2020, doi: 10.1016/j.ces.2020.115912.
[23] A. A. Jasim, A. J. Sultan, and M. H. Al-Dahhan, "Influence of heat-exchanging tubes diameter on the gas holdup and bubble dynamics in a bubble column," *Fuel*, vol. 236, no. September 2018, pp. 1191–1203, 2019, doi: 10.1016/j.fuel.2018.09.049.
[24] N. Iraqi, B. Using, R. Surface, and M. Isotherm, "Adsorption of Blue Cationic Thiazine Dye from Synthetic Wastewater by Adsorption of Blue Cationic Thiazine Dye from Synthetic Wastewater by Natural Iraqi Bentonite Using Response Surface Methodology : Isotherm, Kinetic, and Thermodynamic Studies," *Chem. Africa*, no. January, 2023, doi: 10.1007/s42250-023-00591-w.
[25] I. H. Khalaf, F. T. Al-sudani, and A. A. Abdulrazak, "Optimization of Congo red dye adsorption from wastewater by a modified commercial zeolite catalyst using response surface modeling approach," *Water Sci. Technol.* |, pp. 1369–1383, 2021, doi: 10.2166/wst.2021.078.
[26] Z. M. Shakor, A. A. Abdulrazak, and A. A. Shuhaib, "Optimization of process variables for hydrogenation of cinnamaldehyde to cinnamyl alcohol over a Pt / SiO 2 catalyst using response surface methodology," no. May 2021, 2022, doi: 10.1080/00986445.2021.1922394.
[27] R. S. Abdulmohsin and M. H. Al-Dahhan, "Impact of internals on the heat-transfer coefficient in a bubble column," *Ind. Eng. Chem. Res.*, vol. 51, no. 7, pp. 2874–2881, 2012, doi: 10.1021/ie2018096.
[28] A. Alzamily, A. Sultan, A. Abdulrahman, and H. Majdi, "Study of the Impact of Tube Configurations on the Local Heat Transfer Coefficient in Mimicked Fischer-Tropsch Bubble Column Reactor," *Processes*,

vol. 10, p. 976, May 2022, doi: 10.3390/pr10050976.
[29] R. S. Abdulmohsin, B. A. Abid, and M. H. Al-Dahhan, "Heat transfer study in a pilot-plant scale bubble column," *Chem. Eng. Res. Des.*, vol. 89, no. 1, pp. 78–84, 2011, doi: 10.1016/j.cherd.2010.04.019.
[30] A. K. Jhawar, "Effects of internals configurations on heat transfer and hydrodynamics in bubble columns-with and without solid particles," *Doctoral Dissertation*, The University of Western Ontario 2011.
[31] A. K. Jhawar and A. Prakash, "Heat transfer in a slurry bubble column reactor: A critical overview," *Ind. Eng. Chem. Res.*, vol. 51, no. 4, pp. 1464–1473, 2012, doi org/10.1021/ie201108b.
[32] M. An, X. Guan, and N. Yang, "Modeling the effects of solid particles in CFD-PBM simulation of slurry bubble columns," *Chem. Eng. Sci.*, vol. 223, p. 115743, 2020, doi: 10.1016/j.ces.2020.115743.
[33] G. Olivieri, M. Elena Russo, M. Simeone, A. Marzocchella, and P. Salatino, "Effects of viscosity and relaxation time on the hydrodynamics of gas–liquid systems," *Chem. Eng. Sci.*, vol. 66, no. 14, pp. 3392–3399, Jul. 2011, doi: 10.1016/j.ces.2011.01.027.
[34] L. Peilong, H. Ruijun, Z. Chenxi, and W. Tiefeng, "Hydrodynamic behaviors of a spouted fluidized bed with a conical distributor and auxiliary inlets for the production of polysilicon with wide-size-distribution particles," *Chem. Eng. Sci.*, vol. 247, p. 117069, 2022, doi: 10.1016/j.ces.2021.117069.